The $Ca_V3.2$ T-Type Ca^{2+} Channel Is Required for Pressure Overload–Induced Cardiac Hypertrophy in Mice

Chien-Sung Chiang,* Ching-Hui Huang,* Hockling Chieng, Ya-Ting Chang, Dory Chang, Ji-Jr Chen, Yong-Cyuan Chen, Yen-Hui Chen, Hee-Sup Shin, Kevin P. Campbell, Chien-Chang Chen

Abstract—Voltage-gated T-type Ca^{2+} channels (T-channels) are normally expressed during embryonic development in ventricular myocytes but are undetectable in adult ventricular myocytes. Interestingly, T-channels are reexpressed in hypertrophied or failing hearts. It is unclear whether T-channels play a role in the pathogenesis of cardiomyopathy and what the mechanism might be. Here we show that the α_{1H} voltage-gated T-type Ca^{2+} channel ($Ca_v3.2$) is involved in the pathogenesis of cardiac hypertrophy via the activation of calcineurin/nuclear factor of activated T cells (NFAT) pathway. Specifically, pressure overload–induced hypertrophy was severely suppressed in mice deficient for $Ca_v3.2$ ($Ca_v3.2^{-/-}$) but not in mice deficient for $Ca_v3.1$ ($Ca_v3.1^{-/-}$). Angiotensin II–induced cardiac hypertrophy was also suppressed in $Ca_v3.2^{-/-}$ mice. Consistent with these findings, cultured neonatal myocytes isolated from $Ca_v3.2^{-/-}$ mice fail to respond hypertrophic stimulation by treatment with angiotensin II. Together, these results demonstrate the importance of $Ca_v3.2$ in the development of cardiac hypertrophy both in vitro and in vivo. To test whether $Ca_v3.2$ mediates the hypertrophic response through the calcineurin/NFAT pathway, we generated $Ca_v3.2^{-/-}$, NFAT-luciferase reporter mice and showed that NFAT-luciferase reporter activity failed to increase after pressure overload in the $Ca_v3.2^{-/-}$/NFAT-Luc mice. Our results provide strong genetic evidence that $Ca_v3.2$ indeed plays a pivotal role in the induction of calcineurin/NFAT hypertrophic signaling and is crucial for the activation of pathological cardiac hypertrophy. **(*Circ Res*. 2009;104:522-530.)**

Key Words: hypertrophy ■ cardiomyopathy ■ T-type Ca^{2+} channel

Hypertrophic growth and remodeling of the adult heart begin as normal compensatory responses to a variety of physiological and pathological stimuli including exercise, pregnancy, pressure overload, hypertension, myocardial infarction, and primary genetic abnormalities.[1–3] Prolonged hypertrophic response may eventually lead to heart failure and death. Pathological hypertrophy is often associated with structural and functional remodeling of the heart. Profound changes in gene expression during pathological cardiac hypertrophy are common, particularly in the case of genes that code for proteins involved in regulating contraction ion channels, for example.[4]

Alterations of intracellular Ca^{2+} handling could lead to abnormal Ca^{2+} signaling cascades, a phenomenon that has been shown to contribute to the pathogenesis of cardiac hypertrophy and heart failure.[5,6] However, the detailed mechanism of how the cardiac myocytes distinguish Ca^{2+} transients that occur at every heartbeat from those meant to trigger intracellular hypertrophic signaling remains largely unknown. Intracellular Ca^{2+} levels could be altered because of either changes in Ca^{2+} release from intracellular organelles or the influx of extracellular Ca^{2+}, and in both cases, this could be attributable to the activities of either ligand- or voltage-activated Ca^{2+} channels. Indeed, ligand-activated Ca^{2+} channels, such as store-operated Ca^{2+} channels, have been implicated in the signaling pathway that leads to cardiac hypertrophy.[7] Candidate proteins for store-operated Ca^{2+} channels, such as transient receptor potential proteins (including TRPC1, TRPC3, and TRPC6), have been shown to act as positive regulators of calcineurin/NFAT-mediated signaling, which drive cardiac hypertrophy both in vitro and in vivo.[8–11]

L-type Ca^{2+} channels are the main voltage-activated Ca^{2+} channels responsible for triggering Ca^{2+}-induced Ca^{2+} release during excitation–contraction coupling. Their role in the development of cardiac hypertrophy remains controversial. In general, the current density of L-type Ca^{2+} channels is either unchanged or slightly elevated when hypertrophy is mild and slightly reduced when hypertrophy is severe.[12–14] Although normally expressed during developmental stages and not expressed in adult cardiac myocytes, T-channels are

Original received August 3, 2008; revision received December 17, 2008; accepted December 18, 2008.

From the Institute of Biomedical Sciences (C.-S.C., C.-H.H., H.C., Y.-T.C., D.C., J.-J.C., Y.-C.C.,Y.-H.C., C.-C.C.), Academia Sinica, Taipei, Taiwan; Graduate Institute of Life Sciences (C.-H.H., C.-C.C.), National Defense Medical Center, Taipei, Taiwan; Center for Neural Science (H.-S.S.), Korea Institute of Science and Technology, Seoul, Korea; and Department of Physiology and Biophysics and Department of Neurology (K.P.C.), Howard Hughes Medical Institute, University of Iowa, Iowa City.

*Both authors contributed equally to the study.

Correspondence to Chien-Chang Chen, Institute of Biomedical Sciences, Academia Sinica, 128 Academia Rd Sec 2, Nankang, Taipei 11529, Taiwan. E-mail ccchen@ibms.sinica.edu.tw

Circulation Research **is available at http://circres.ahajournals.org** **DOI: 10.1161/CIRCRESAHA.108.184051**

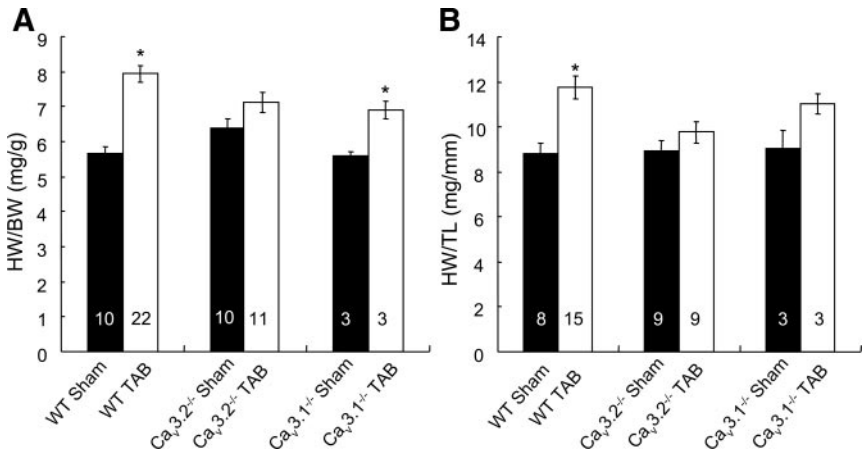

Figure 1. Ca$_v$3.2 is required for TAB-induced cardiac hypertrophy. A, Quantitation of HW/BW ratio in mice that were sham-operated or subjected to TAB for 2 weeks. B, Quantitation of HW/tibial length ratio in mice that were sham-operated or subjected to TAB for 2 weeks. Numbers of mice used in each group are shown. *$P<0.001$ relative to sham-operated controls.

reexpressed after development of pathological hypertrophy, in the postinfarction heart, and during stimulation with certain hormones.[15–23] The pore-forming subunits of T-channels are encoded by 3 genes, Ca$_v$3.1, -3.2 and -3.3,[24–26] and both Ca$_v$3.1 and Ca$_v$3.2 are present in cardiac tissue.[27–29] Mice lacking Ca$_v$3.1 T-channels display abnormal sinoatrial node pacemaker activity and atrioventricular conduction,[30] whereas mice lacking Ca$_v$3.2 exhibit recurrent coronary vasospasms.[31] Ca$_v$3.1 and Ca$_v$3.2 have been reported to be upregulated in various animal models following cardiac hypertrophy.[18,19,22] However, the physiological role of T-channel reexpression under these conditions is unclear.

In this study, we aimed to determine whether Ca$_v$3.2 T-channels are involved in the development of pathological cardiac hypertrophy and whether the calcineurin–NFAT pathway is downstream of Ca$_v$3.2 T-channels during cardiac hypertrophy. Using Ca$_v$3.2$^{-/-}$ and Ca$_v$3.1$^{-/-}$ mice, we show that Ca$_v$3.2 but not Ca$_v$3.1 T-channels are required for the development of cardiac hypertrophy induced either by pressure overload and angiotensin (Ang) II treatment in vivo and in vitro. We also discover that the T-channel blocker ethosuximide could prevent the development of pressure overload–induced cardiac hypertrophy in wild-type (WT) mice, and that the stimulation of NFAT signaling in response to pressure overload requires the presence of Ca$_v$3.2. Overall, our results demonstrate that Ca$_v$3.2 T-channels regulate pathogenic cardiac hypertrophy in vivo by activating the calcineurin–NFAT signaling cascade.

Materials and Methods

Animals were kept under specific pathogen-free conditions, and all procedures performed were approved by the Institutional Animal Care and Use Committee of Academia Sinica, Taiwan. An expanded Materials and Methods section detailing the methods and protocols used in the present study is available in the online data supplement at http://circres.ahajournals.org.

Results

Impaired Cardiac Hypertrophy in Ca$_v$3.2$^{-/-}$ but Not Ca$_v$3.1$^{-/-}$ Mice Following Transverse Aortic Banding

Although an association between T-channel reexpression and cardiac hypertrophy has been established, an in vivo loss-of-function approach to causality has not previously been undertaken. In this study, we compared the extent of cardiac hypertrophy in WT, Ca$_v$3.2$^{-/-}$, and Ca$_v$3.1$^{-/-}$ mice following pressure overload to determine the role of T-channels in the development of cardiac hypertrophy. Measurement of the Doppler flow pressure gradient (in meters per second) following constriction of the transverse aorta (Table I in the online data supplement) indicated that WT, Ca$_v$3.2$^{-/-}$, and Ca$_v$3.1$^{-/-}$ mice were subjected to a comparable pressure load. Notably, Ca$_v$3.2$^{-/-}$ mice or their sham-operated animals have a smaller body size relative to those age-matched WT mice (supplemental Table I), thus resulting in a higher ratio of heart weight/body weight (HW/BW) (in milligrams per gram) (Figure 1A and supplemental Table I). In WT and Ca$_v$3.1$^{-/-}$ mice, by 2 weeks following transverse aortic banding (TAB) treatment, the HW/BW ratio had increased significantly by 39.9% and 22.9%, respectively, relative to that in age-matched, sham-operated WT and Ca$_v$3.1$^{-/-}$ mice ($P<0.001$). In Ca$_v$3.2$^{-/-}$ mice, by contrast, the HW/BW ratio in the banded animals and their sham controls did not differ significantly ($P=0.07$) (Figure 1A). Measurement and comparison of another hypertrophy index, the HW/tibial length (in milligrams per millimeter) ratio, across groups yielded similar results (Figure 1B). We also measured the blood pressure of WT and Ca$_v$3.2$^{-/-}$ mice at both basal and 2 weeks after TAB. There is no significant difference in blood pressure between WT and Ca$_v$3.2$^{-/-}$ mice after TAB (109±3 for WT versus 109±2 mm Hg for Ca$_v$3.2$^{-/-}$).

Histological examination of hearts also showed a significant increase in ventricular wall thickness in the banded WT mice but less in the banded Ca$_v$3.2$^{-/-}$ mice (Figure 2A). One hallmark of cardiac hypertrophy is the enlargement of individual myocytes, and thus cardiomyocyte hypertrophy was also assessed at the cellular level. TAB treatment was found to lead to a significant increase in the cardiac myocyte cross-sectional diameter (in microns) by 23% in banded WT mice compared with sham-operated controls ($P<0.001$) (Figure 2B). In contrast, there was no significant change in the myocyte cross-sectional diameter from the banded Ca$_v$3.2$^{-/-}$ mice compared with the sham-operated controls ($P=0.1$). The progression to the cardiomyopathy is accompanied by increased fibrosis. Ca$_v$3.2$^{-/-}$ mice have been shown to display focal myocardial fibrosis caused by abnormal coronary function.[31] Indeed, there was more fibrosis in sham-

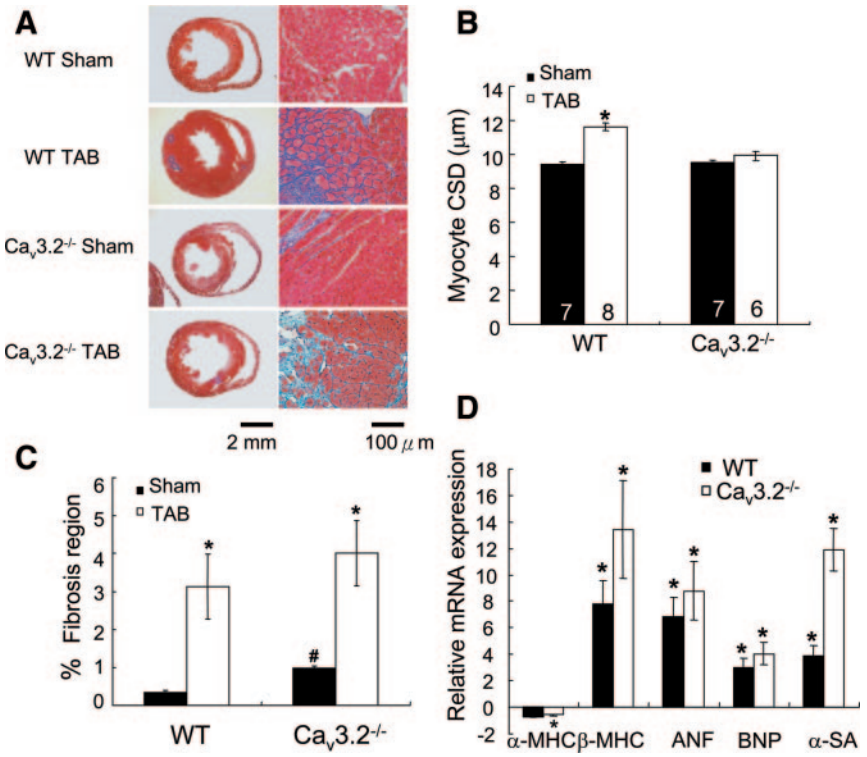

Figure 2. Reduced cardiomyocyte growth in $Ca_v3.2^{-/-}$ mice induced by TAB. A, Mason's trichromic staining of cross-sectioned hearts from WT and $Ca_v3.2^{-/-}$ mice subjected to TAB for 2 weeks. B, Myocyte cross-sectional diameter (CSD) measured from cross-sectioned hearts from WT and $Ca_v3.2^{-/-}$ mice subjected to TAB for 2 weeks (total 250 to 400 cells for each heart; numbers of mice used in each group are shown). *$P<0.001$ relative to sham-operated controls. C, Morphometric quantitation of fibrosis in sham- and TAB-operated mice. *$P<0.05$ relative to sham-operated controls for the same genotype, #$P<0.05$ for WT vs $Ca_v3.2^{-/-}$. Data reflect measurements for at least 4 animals per group. D, Real-time RT-PCR analysis of expression of the hypertrophic markers α-MHC, β-MHC, ANF, BNP, and α-SA after 2 weeks of TAB treatment (n=3 to 5, for each group). The mean normalized value for the expression of each gene in their sham-operated hearts is defined as 1. *$P<0.05$ vs sham-operated.

operated $Ca_v3.2^{-/-}$ mice than those in WT mice (Figure 2C). After TAB treatment, there was a marked increase in myocardial fibrosis in both WT and $Ca_v3.2^{-/-}$ mice, and no significant difference in myocardial fibrosis between WT and $Ca_v3.2^{-/-}$ mice was observed after TAB (Figure 2A and 2C).

Because cardiac hypertrophy is frequently accompanied by a reexpression of the cardiac fetal genes, we examined the expression of atrial natriuretic factor (ANF), brain natriuretic peptide (BNP), α-myosin heavy chain (α-MHC), β-myosin heavy chain (β-MHC), and skeletal α-actin (α-SA) in the banded WT and $Ca_v3.2^{-/-}$ hearts using real-time quantitative PCR. As expected, ANF, BNP, β-MHC, and α-SA were significantly upregulated in the banded WT heart, whereas α-MHC was downregulated (Figure 2D). Notably, despite the attenuation of hypertrophy in the $Ca_v3.2^{-/-}$ heart, the expression of ANF, BNP, β-MHC, and α-SA were also upregulated and the expression of α-MHC was downregulated under these conditions ($P<0.05$), suggesting that $Ca_v3.2$ channels are not involved in the reexpression of these fetal genes during pathological hypertrophy.

We also performed serial echocardiography to characterize the change in cardiac structure and function after pressure overload. Left ventricle mass (LVM) and the LVM/BW ratio had increased significantly in the banded WT and $Ca_v3.1^{-/-}$ mice at 2 and 4 weeks after banding relative to animals at basal condition. In $Ca_v3.2^{-/-}$ mice, however, LVM and the LVM/BW ratio did not increase at all in 2-week banded $Ca_v3.2^{-/-}$ mice, although a modest but significant increase in LVM/BW was observed at 4 weeks after banding (Figure 3A and 3B and supplemental Table I). The hypertrophic response in banded $Ca_v3.2^{-/-}$ mice was markedly reduced compared to that in banded WT animals for the same period, whereas hypertrophic response in banded $Ca_v3.1^{-/-}$ mice was comparable to that in banded WT animals (Figure 3B). Cardiac function, as indicated by the percentage of fractional shortening, did not show significant difference in WT at basal or after 2- and 4-week TAB, nor did it show a difference in $Ca_v3.2^{-/-}$ or $Ca_v3.1^{-/-}$ mice. Fractional shortening was comparable among WT, $Ca_v3.2^{-/-}$, and $Ca_v3.1^{-/-}$ mice when subjected to the same period of TAB (Figure 3C).

Compromised Ang II–Induced Cardiac Hypertrophy in $Ca_v3.2^{-/-}$ Mice

Pressure overload–induced cardiac hypertrophy is mediated in part via the mechanical stress–dependent and neuroendocrine factor–dependent pathways, such as those mediated by Ang II and endothelin 1.[1,5] To test whether Ang II can induce cardiac hypertrophy in $Ca_v3.2^{-/-}$ mice, Ang II was continuously infused into WT and $Ca_v3.2^{-/-}$ mice for 2 weeks. Ang II infusion markedly increased systemic blood pressure in both WT and $Ca_v3.2^{-/-}$ mice, suggesting that $Ca_v3.2^{-/-}$ mice, although having a compromised vascular function, remain functionally intact in response to Ang II–induced hypertension (Figure 4A). As in the case of the TAB results, Ang II treatment led to a significant increase in the LVM/BW in WT but not in $Ca_v3.2^{-/-}$ mice (Figure 4B). After 2 weeks of Ang II treatment, the ratio of LVM/BW increased significantly by 33.6% in WT mice ($P<0.01$), whereas the ratio did not change significantly in $Ca_v3.2^{-/-}$ mice.

To determine whether the reduced cardiac hypertrophy observed in $Ca_v3.2^{-/-}$ mice was attributable to the lack of $Ca_v3.2$ channels in cardiac myocytes, we isolated and cultured neonatal cardiac myocytes from WT and $Ca_v3.2^{-/-}$ mice and tested their hypertrophic responses to Ang II in vitro. Ang II significantly increased the surface area of only the WT cardiac myocytes (by 17.8%, $P<0.001$) but not that

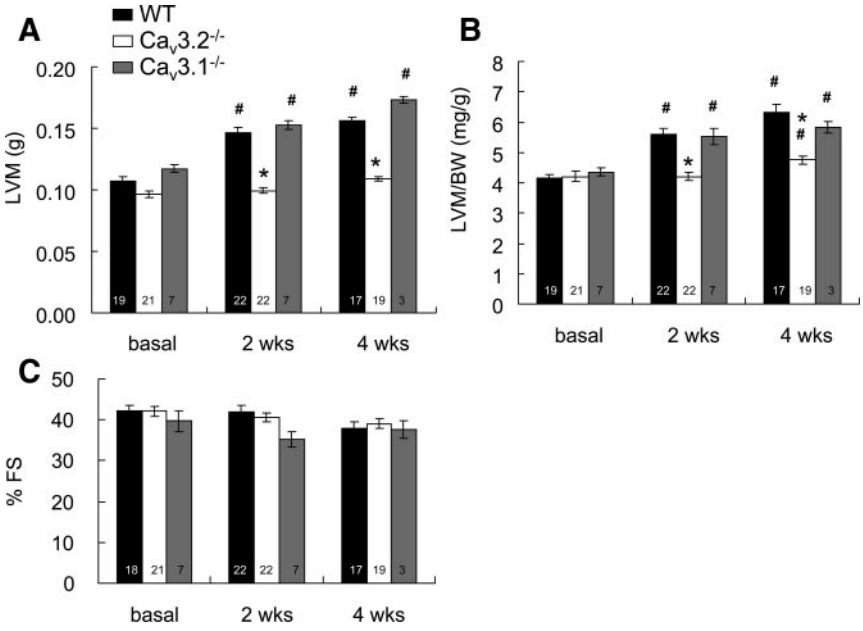

Figure 3. Reduced cardiac hypertrophic response in Ca$_v$3.2$^{-/-}$ but not Ca$_v$3.1$^{-/-}$ mice following TAB treatment. A and B, LVM (A) and LVM/BW ratio (B). C, Percentage of fractional shortening (% FS) from WT, Ca$_v$3.2$^{-/-}$, and Ca$_v$3.1$^{-/-}$ mice by serial echocardiography during pressure overload. *P<0.05 Ca$_v$3.2$^{-/-}$ vs WT at the same time point. #P<0.05 TAB-treated vs basal group for the same genotype. LVM increased by 37% and 46% in WT mice vs 5% and 15% in Ca$_v$3.2$^{-/-}$ mice and 30% and 48% in Ca$_v$3.1$^{-/-}$ mice 2 and 4 weeks, respectively, after TAB. Similarly, LVM/BW increased by 35% and 53% in WT mice vs 4% and 15% in Ca$_v$3.2$^{-/-}$ mice and 27% and 34% in Ca$_v$3.1$^{-/-}$ mice 2 and 4 weeks, respectively, after TAB. Numbers of mice used in each group are shown.

of the Ca$_v$3.2$^{-/-}$ cardiac myocytes (Figure 5A and 5B). RT-PCR analysis indicated that neonatal WT mouse myocytes express all 3 Ca$_v$3 channel isoforms (Figure 5C). On Ang II stimulation, only *Ca$_v$3.2* mRNA but not *Ca$_v$3.1* or *Ca$_v$3.3* mRNA was markedly increased in neonatal WT myocytes (Figure 5C and 5D), whereas the level of *Ca$_v$3.1* and *Ca$_v$3.3* mRNA expression remained unchanged in neonatal Ca$_v$3.2$^{-/-}$ myocytes. Our in vivo and in vitro studies suggest the activation of Ca$_v$3.2 channels is important to the development of cardiac hypertrophy.

Inhibition of T-type Ca^{2+} Channels Blunts Cardiac Hypertrophy

Because pressure overload– and Ang II–induced cardiac hypertrophy was blunted in Ca$_v$3.2$^{-/-}$ mice, we tested whether cardiac hypertrophy could be inhibited by blocking T-channels. Because no specific T-channel blocker is available commercially, we chose ethosuximide, which has been used to block T-channels in vitro and in vivo,[32–34] to test our hypothesis. WT mice were subjected to TAB and concurrently infused with ethosuximide for 2 weeks. As shown in Figure 6A, TAB-induced cardiac hypertrophy (as assessed by the LVM/BW ratio) was significantly attenuated in the ethosuximide-treated groups by 15.6% (P<0.01), when compared to the corresponding vehicle-treated group. We also found that ethosuximide can reduce Ang II–mediated increase of LVM/BW ratio by 19% (P<0.05) (Figure 6B). These data demonstrate that blocking T-channels in WT mice can reduce cardiac hypertrophy induced by either pressure overload or treatment with Ang II.

Electrophysiological Examinations of Ca^{2+} Currents From Acutely Isolated Left Ventricular Myocytes

Reappearance of the T-current has been observed in hypertrophied ventricular cells in the association with pressure overload in feline[16] and rat.[18,19] Using the whole-cell patch-clamp technique, we examined whether T-type Ca^{2+} current (T-current) reappeared in the left ventricular myocytes from 2-week TAB WT mice. Small but detectable T-currents were recorded in WT myocytes after TAB, whereas they are not detectable or very small in WT myocytes following sham operation (Figure 7) (at −40 mV, −0.64±0.17 pA/pF for TAB [n=5] and −0.11±0.02 pA/pF for sham [n=12]; P<0.05). The T-current recorded in WT myocytes after TAB was peaked at approximately −40 mV, and bath application of 100 μmol/L Ni^{2+} caused a rapid reduction of T-current amplitude to ≈75% of control, indicating relatively high sensitivity of the current to Ni^{2+} (Figure 7B, inset). The L-type Ca^{2+} current (L-current) density was similar in sham-operated WT myocytes compared

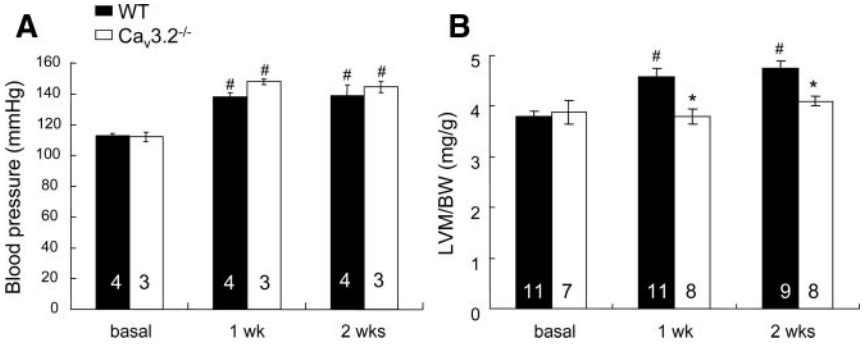

Figure 4. Ang II fails to induce cardiac hypertrophy in Ca$_v$3.2$^{-/-}$ mice. A, Blood pressure of WT and Ca$_v$3.2$^{-/-}$ mice before and after stimulation with continuous Ang II infusion. #P<0.05 treatment vs its basal group for the same genotype. B, LVM/BW, as measured by echocardiography, after WT or Ca$_v$3.2$^{-/-}$ mice were subjected to continuous Ang II infusion. Numbers of mice used in each group are shown. #P<0.01 treatment vs its basal group for the same genotype. *P<0.05 Ca$_v$3.2$^{-/-}$ vs WT at the same time point.

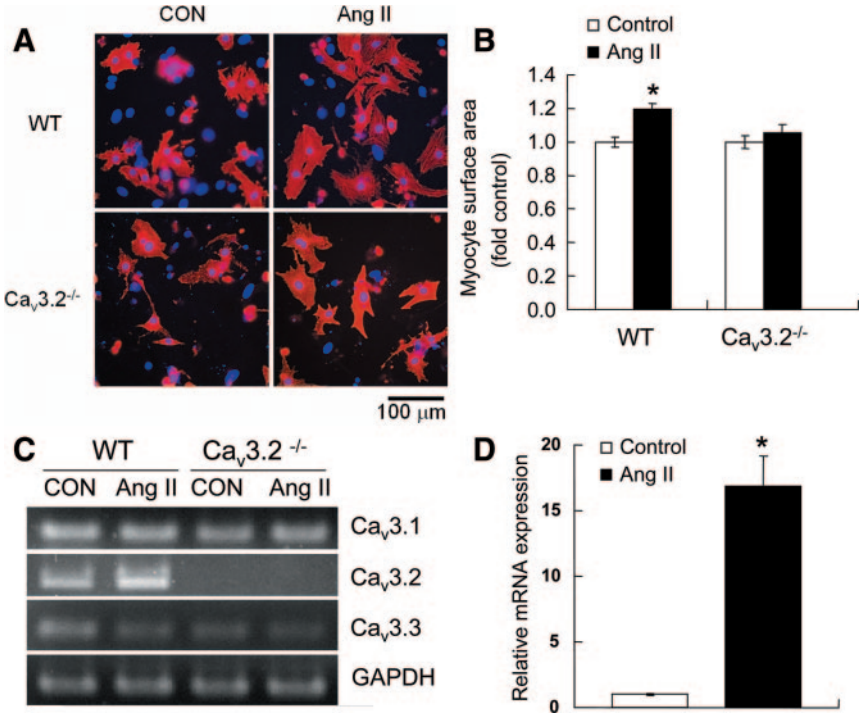

Figure 5. Ang II fails to induce hypertrophy of neonatal cardiomyocytes isolated from $Ca_v3.2^{-/-}$ mice. A, Neonatal cardiomyocytes isolated from WT or $Ca_v3.2^{-/-}$ mice were either left untreated or treated with 100 μmol/L Ang II for 48 hours. Neonatal cardiomyocytes were identified by α-actinin antibody staining (red signal) and nuclei by DAPI staining (blue signal). B, Ang II treatment increased cell surface area in WT, but not $Ca_v3.2^{-/-}$, cardiomyocytes. Two hundred to 300 random cells from 3 independent experiments in WT and $Ca_v3.2^{-/-}$ mice were measured. *$P<0.001$ vs control for the same genotype. C, The levels of $Ca_v3.1$, $Ca_v3.2$, and $Ca_v3.3$ mRNA from neonatal WT and $Ca_v3.2^{-/-}$ myocytes were analyzed by RT-PCR with or without Ang II stimulation for 48 hours. D, Real-time RT-PCR analysis of the expression of $Ca_v3.2$ in neonatal WT myocytes after Ang II treatment for 48 hours. *$P<0.05$ Ang II vs control.

with sham-operated $Ca_v3.2^{-/-}$ myocytes (peak inward at 10 mV, -7.83 ± 0.49 pA/pF for WT sham [n=14] and -8.09 ± 0.48 pA/pF for knockout sham [n=15]). After TAB, there is no significant change in the L-current density in both WT and $Ca_v3.2^{-/-}$ myocytes (peak inward at 10 mV, -8.23 ± 0.52 pA/pF for WT TAB [n=15] and -7.98 ± 0.41 pA/pF for knockout TAB [n=15]) (Figure 7C). It has been reported that the reduction of the L-current by continuous infusion of L-channel blocker[35] or the knockdown of L-channel accessory β subunit[36] alleviates hypertrophic response. Our data rule out the possibility that blunted hypertrophy response in banded $Ca_v3.2^{-/-}$ mice results from the downregulation of L-type Ca^{2+} currents.

Calcineurin–NFAT Signaling Is Not Activated in $Ca_v3.2^{-/-}$ Mice After Pressure Overload

The calcineurin–NFAT signaling pathway is important in regulating the development of cardiac hypertrophy and the associated changes in gene expression. It is thus possible that the reexpression of $Ca_v3.2$ channels can activate the calcineurin–NFAT signaling pathway during cardiac hypertrophy. To test this possibility, we first examined whether the expression of $Ca_v3.2$ could enhance the NFAT–luciferase activity in HEK293 cells. It has been shown that increased extracellular Ca^{2+} concentration to 10 mmol/L could induce Ca^{2+} influx via the $Ca_v3.2$ T-channels that open at the resting membrane potential of a HEK293 cell (ie, window current).[37,38] As shown in Figure 8A, 10 mmol/L Ca^{2+} significantly increased the NFAT–luciferase reporter activity relative to that of cells transfected with control vehicle and T-channel blocker mibefradil effectively blocked NFAT–luciferase activity triggered by calcium. We further investigated whether calcineurin–NFAT signaling is intact in the $Ca_v3.2^{-/-}$ heart by crossing the $Ca_v3.2^{-/-}$ mice with a NFAT–luciferase (Luc) reporter transgenic mice.[39] The basal level of NFAT-Luc reporter activity in the left ventricle was not significantly different between WT/NFAT-Luc and $Ca_v3.2^{-/-}$/NFAT-Luc mice (Figure 8B). As expected, cardiac NFAT-Luc reporter activity increased significantly by 2.5-fold ($P<0.001$) 2 weeks after TAB in the WT/NFAT-Luc mice. In contrast, there

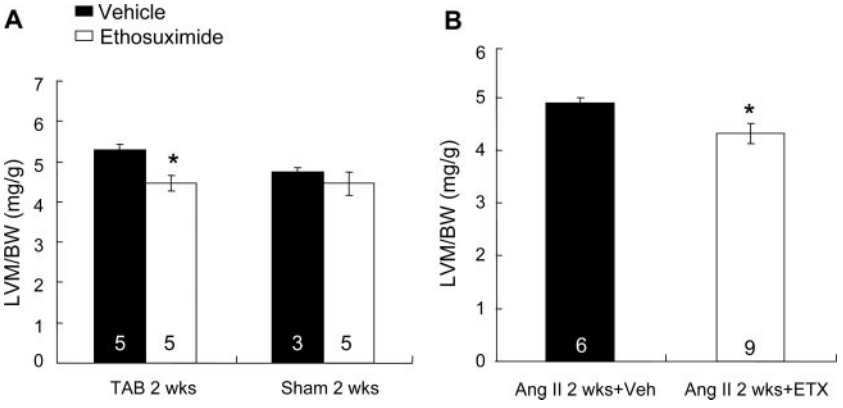

Figure 6. Inhibition of T-type Ca^{2+} channel by ethosuximide treatment prevents cardiac hypertrophy in WT mice. A, LVM/BW ratio in mice treated with vehicle or ethosuximide immediately following TAB surgery. The duration of the treatment lasted for 2 weeks. *$P<0.01$ vs vehicle in the same group. B, LVM/BW ratio in mice treated with Ang II and Ang II plus ethosuximide for 2 weeks. *$P<0.05$ vs vehicle group. Numbers of mice used in each group are shown.

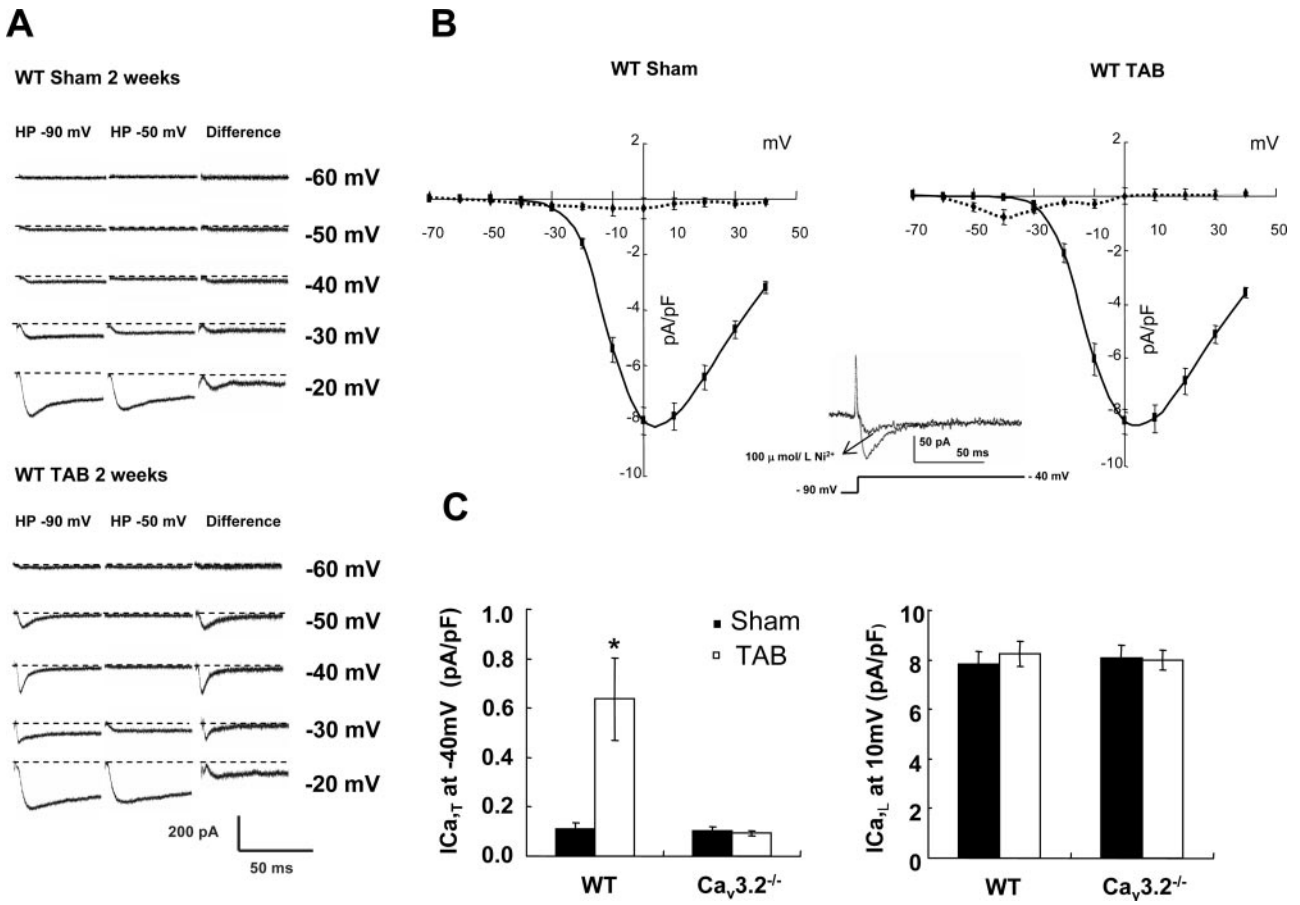

Figure 7. T-type Ca^{2+} currents are upregulated in left ventricular myocytes from banded WT hearts. A, Ca^{2+} currents were recorded in left ventricular myocytes from 2-week sham- or TAB-operated mouse hearts. Traces of T-type Ca^{2+} current correspond to the difference between currents recorded for step polarization from holding potentials (HP) of −90 and −50 mV. Horizontal lines indicate the 0 current level. B, Current–voltage relationships of L-currents (solid line) and T-currents (dashed line) obtained in myocytes from 2-week sham- or TAB-operated mouse hearts. Inset shows the effect of 100 μmol/L Ni^{2+} on T-current in a myocyte from a 2-week TAB WT heart. C, T-type ($I_{Ca,T}$) (at −40 mV) and L-type Ca^{2+} current density ($I_{Ca,L}$) (at 10 mV) in myocytes from 2-week sham- and TAB-operated WT and Ca$_v$3.2$^{-/-}$ mice. The *y* axis depicts absolute ionic current density induced. Data reflect measurements from 2 to 3 animals per group. *P<0.05 vs WT sham.

was no significant change in luciferase reporter activity 2 weeks after TAB in the Ca$_v$3.2$^{-/-}$/NFAT-Luc mice. We also measured the protein levels of total calcineurin A from the left ventricles of WT/NFAT-Luc and Ca$_v$3.2$^{-/-}$/NFAT-Luc mice and found no difference (Figure 8C). These data suggest that Ca$_v$3.2 channels are important in the activation of calcineurin–NFAT signaling and that the lack of NFAT–luciferase activity in the Ca$_v$3.2$^{-/-}$/NFAT-Luc mice is not attributable to a secondary change in the level of calcineurin A protein. To determine whether there could be any interaction between Ca$_v$3.2 T-channels and calcineurin, we performed coimmunoprecipitation experiments in vitro. We coexpressed vectors containing FLAG-Ca$_v$3.2 or FLAG-Ca$_v$3.1 and calcineurin in HEK293 cells. As shown in Figure 8D, calcineurin can be coimmunoprecipitated with FLAG-Ca$_v$3.2. In contrast, there is no detectable calcineurin in the FLAG vector control and a much weaker band of calcineurin coimmunoprecipitated with FLAG-Ca$_v$3.1 despite a larger amount of FLAG-Ca$_v$3.1 in the input lysates. The results suggest that the Ca$_v$3.2 T-channels can interact with calcineurin in HEK293 cells in vitro and could play a role in the hypertrophic signaling.

Discussion

Although T-type Ca^{2+} channels have been previously implicated in the growth of cardiac tissues and in the pathogenesis associated with Ca^{2+} overload and cardiomyopathy-related arrhythmias,[16–23] little is known about the mechanism whereby these channels act. Using Ca$_v$3.2$^{-/-}$ and Ca$_v$3.1$^{-/-}$ mice, we were able to demonstrate that Ca$_v$3.2 T-channels are required for hypertrophic response to mechanical stress and Ang II infusion.

Upregulation of *Ca$_v$3.1* mRNA was observed in hypertrophied ventricles and failure-stage hearts in rats.[19,22] Paradoxically, in the hypertrophied rat hearts, the increased T-type calcium currents from left ventricular myocytes showed relatively high nickel sensitivity, a feature peculiar to Ca$_v$3.2 channel–generated currents.[18] A recent study reported that, in the ventricular septum of the aortic banded mouse heart, *Ca$_v$3.1* mRNA expression decreased, whereas *Ca$_v$3.2* mRNA expression was comparable to that in sham-operated control hearts.[40] These conflicting results may reflect the different genetic backgrounds of experimental animals and the surgical protocols whereby cardiac hypertrophy was induced. Never-

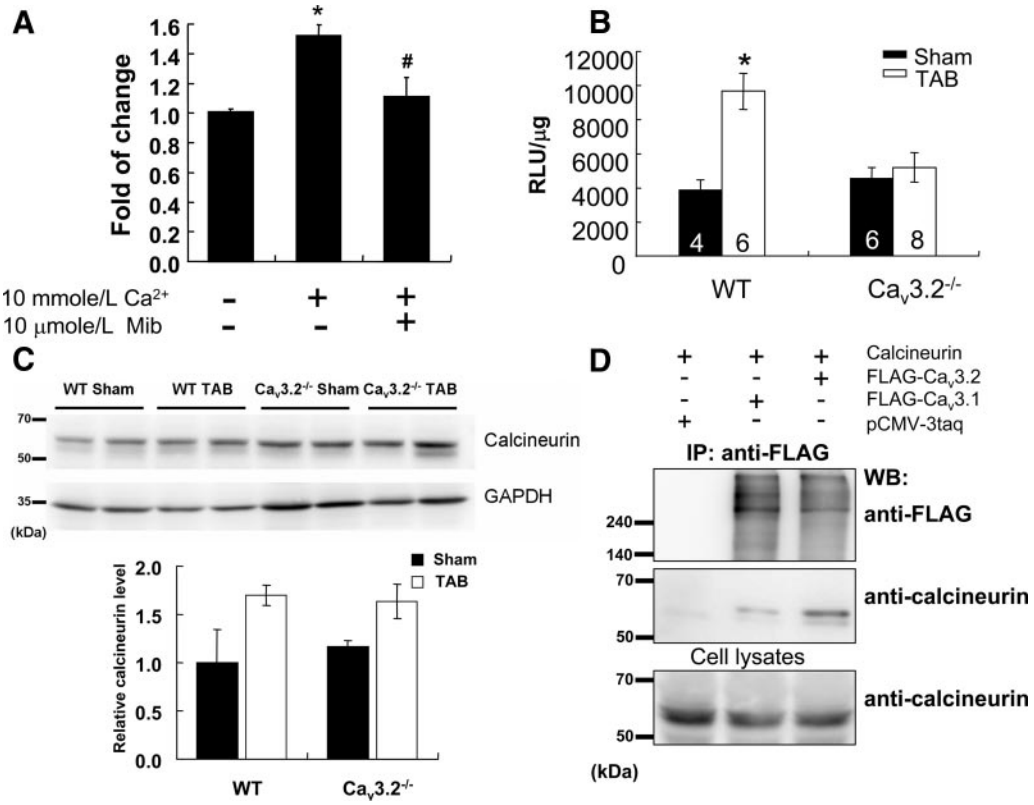

Figure 8. Pressure overload fails to boost NFAT activation in $Ca_v3.2^{-/-}$/NFAT-Luc mice. A, In vitro studies examine the effect of $Ca_v3.2$ overexpression on Ca^{2+}-stimulating NFAT activation in HEK293 cells. *$P<0.05$ vs untreated control, #$P<0.05$ vs 10 mmol/L Ca^{2+}-treated cells. B, Left ventricular NFAT-luciferase reporter activity assessed after 2 weeks of TAB in WT/NFAT-Luc and $Ca_v3.2^{-/-}$/NFAT-Luc mice. Numbers of mice used in each group and NFAT reporter activity are shown. *$P<0.001$ vs WT sham. C, Western blotting for total calcineurin A (CnA) from left ventricle tissue of WT/ NFAT-Luc and $Ca_v3.2^{-/-}$/NFAT-Luc mice. GAPDH serves as a loading control. Quantitations of CnA expression are shown at the bottom. D, Coimmunoprecipitation of $Ca_v3.2$ channels and calcineurin in vitro.

theless, these studies failed to clarify whether the reexpression of T-channels is the consequence of cardiac remodeling in pathological states or whether the reexpressed T-channels, instead, initiate cardiac remodeling. Our demonstrations that nickel sensitive T-currents reappear in WT mice after TAB and T-channel blocker ethosuximide can blunt the development of cardiac hypertrophy induced by pressure overload or Ang II in WT animals suggest that $Ca_v3.2$ T-channels are indeed important in the initiation of pressure overload– and Ang II–induced cardiac hypertrophy in mice.

Pathological cardiac hypertrophy is commonly accompanied by myocyte enlargement, activation of a fetal program of cardiac gene expression, and fibrosis.[5] Our findings that banded $Ca_v3.2^{-/-}$ mice were resistant to cardiac hypertrophy but not fetal gene activation and fibrosis suggest that *$Ca_v3.2$* is not necessary for these pathological features during cardiac remodeling on stress. There are several reports showing that reexpression of cardiac fetal genes is not associated with cardiac hypertrophy but rather with the pathological features. For example, *SCN5A* heterozygous mice show upregulation of β-MHC and α-SA with no hypertrophy.[41] Increased level of ANF expression is associated with tissue pathology but not necessary to the degree of cardiac hypertrophy.[42] Intriguingly in a genetic mouse model with a yellow fluorescent protein–β-MHC fusion gene, reexpression of β-MHC has been found to occur predominantly in myocytes associated with regions with perivascular and interstitial fibrosis during hypertrophy.[43]

The Ca^{2+}/calmodulin serine/threonine protein phosphatase calcineurin plays a central role in the development of pathological cardiac hypertrophy. Our studies show that cardiac hypertrophy responses are impaired in $Ca_v3.2^{-/-}$ mice, NFAT activity in these mice is blunted following 2-week TAB, and the T-currents reexpress in myocytes from banded WT mice, implying $Ca_v3.2$ T-channels are also involved in the activation of calcineurin–NFAT signaling and essential for pathological cardiac hypertrophy. Although a proximal relationship among calcineurin–NFAT, Ca^{2+} handling, and downstream effectors remains largely unclear, our coimmunoprecipitation work shows that the $Ca_v3.2$ T-channels could associate with calcineurin and thus play a role in the hypertrophic signaling. Several recent studies have demonstrated that TRPC1, TRPC3, and TRPC6 are involved in calcineurin/NFAT activation and cardiac hypertrophy in rodent models.[8–11] TRPC6 and TRPC3 transgenic mice exhibit cardiomyopathy associated with increased NFAT activity and with an increased susceptibility to stimulation by pressure overload.[8,11] Furthermore, the promoter region of TRPC6 contains 2 NFAT binding sites, which suggests that positive feedback is involved in the regulation of the calcineurin–NFAT–TRPC6 signaling pathway.[11] We hypothesized that reexpressed $Ca_v3.2$ might induce cardiac hypertrophy by activating the calcineurin–NFAT pathway. Indeed, our analysis of mice harboring a transgenic NFAT-Luc reporter showed that

the activation of NFAT is blunted in the $Ca_v3.2^{-/-}$ left ventricle following pressure overload. The notion is also upheld by the recent in vitro study showing that T-type Ca^{2+} blockers, kurtoxin and efonidipine, could prevent bovine serum–induced neonatal mouse cardiomyocyte hypertrophy through an inhibition of calcineurin–NFAT activation.[44] Interestingly, TRPC6 transcript levels have been reported to increase 3 weeks after TAB.[11] Moreover, following aortic banding in the rat, there is a 2-day delay in the association of calcineurin with calmodulin,[45] which coincides with the time point at which cardiac NFAT-Luc reporter activity is upregulated in mice.[39] This result suggests that calcineurin is activated as early as 2 days after stimulation. It is possible that hypertrophic stimuli lead to rapid activation of $Ca_v3.2$ channels, which then activate calcineurin–NFAT signaling at the initial stage of hypertrophic development, and that this, in turn, induces the sustained hypertrophic responses that are associated with TRPC channel upregulation.

In summary, in using a molecular genetic approach, we have demonstrated that $Ca_v3.2$ plays an important role in the development of cardiac hypertrophy induced by aortic banding and Ang II infusion and that $Ca_v3.2$ is required for activation of the calcineurin/NFAT pathway. The next steps in better understanding the development of cardiac hypertrophy include further evaluating the role of $Ca_v3.2$ inhibition in other genetic and acquired models of cardiac hypertrophy and identifying any $Ca_v3.2$-associated molecules that are involved in the regulation of cardiac hypertrophy.

Acknowledgments

We thank Dr Jeffery D. Molkentin (University of Cincinnati) for kindly providing us the NFAT-Luc reporter mice. We are grateful to the Pathology Core at the Institute of Biomedical Sciences, Academia Sinica, Taiwan for technical assistance.

Sources of Funding

C.-C.C. was supported by grants from the Academia Sinica (AS95IBMS6) and the National Science Council, Taiwan (95-2320-B-001-030, 95-2320-B-001-036). C.-S.C. was a recipient of postdoctoral fellowship from Academia Sinica, Taiwan.

Disclosures

None.

References

1. Ahmad F, Seidman JG, Seidman CE. The genetic basis for cardiac remodeling. *Annu Rev Genomics Hum Genet*. 2005;6:185–216.
2. McMullen JR, Izumo S. Role of the insulin-like growth factor 1 (IGF1)/phosphoinositide-3-kinase (PI3K) pathway mediating physiological cardiac hypertrophy. *Novartis Found Symp.* 2006;274:90–111.
3. Eghbali M, Wang Y, Toro L, Stefani E. Heart hypertrophy during pregnancy: a better functioning heart? *Trends Cardiovasc Med*. 2006;16:285–291.
4. Zwadlo C, Borlak J. Disease-associated changes in the expression of ion channels, ion receptors, ion exchangers and Ca(2+)-handling proteins in heart hypertrophy. *Toxicol Appl Pharmacol*. 2005;207:244–256.
5. Frey N, Olson EN. Cardiac hypertrophy: the good, the bad, and the ugly. *Annu Rev Physiol*. 2003;65:45–79.
6. Wehrens XH, Lehnart SE, Marks AR. Intracellular calcium release and cardiac disease. *Annu Rev Physiol*. 2005;67:69–98.
7. Hunton DL, Lucchesi PA, Pang Y, Cheng X, Dell'Italia LJ, Marchase RB. Capacitative calcium entry contributes to nuclear factor of activated T-cells nuclear translocation and hypertrophy in cardiomyocytes. *J Biol Chem*. 2002;277:14266–14273.
8. Nakayama H, Wilkin BJ, Bodi I, Molkentin JD. Calcineurin-dependent cardiomyopathy is activated by TRPC in the adult mouse heart. *FASEB J*. 2006;20:1660–1670.
9. Ohba T, Watanabe H, Murakami M, Takahashi Y, Iino K, Kuromitsu S, Mori Y, Ono K, Iijima T, Ito H. Upregulation of TRPC1 in the development of cardiac hypertrophy. *J Mol Cell Cardiol*. 2007;42:498–507.
10. Onohara N, Nishida M, Inoue R, Kobayashi H, Sumimoto H, Sato Y, Mori Y, Nagao T, Kurose H. TRPC3 and TRPC6 are essential for angiotensin II-induced cardiac hypertrophy. *EMBO J*. 2006;25:5305–5316.
11. Kuwahara K, Wang Y, McAnally J, Richardson JA, Bassel-Duby R, Hill JA, Olson EN. TRPC6 fulfills a calcineurin signaling circuit during pathologic cardiac remodeling. *J Clin Invest*. 2006;116:3114–3126.
12. Mukherjee R, Spinale FG. L-type calcium channel abundance and function with cardiac hypertrophy and failure: a review. *J Mol Cell Cardiol*. 1998;30:1899–1916.
13. Yatani A, Honda R, Tymitz KM, Lalli MJ, Molkentin JD. Enhanced Ca2+ channel currents in cardiac hypertrophy induced by activation of calcineurin-dependent pathway. *J Mol Cell Cardiol*. 2001;33:249–259.
14. Wang Z, Kutschke W, Richardson KE, Karimi M, Hill JA. Electrical remodeling in pressure-overload cardiac hypertrophy: role of calcineurin. *Circulation.* 2001;104:1657–1663.
15. Xu XP, Best PM. Increase in T-type calcium current in atrial myocytes from adult rats with growth hormone-secreting tumors. *Proc Natl Acad Sci U S A*. 1990;87:4655–4659.
16. Nuss HB, Houser SR. T-type Ca2+ current is expressed in hypertrophied adult feline left ventricular myocytes. *Circ Res*. 1993;73:777–782.
17. Sen L, Smith TW. T-type Ca2+ channels are abnormal in genetically determined cardiomyopathic hamster hearts. *Circ Res*. 1994;75:149–155.
18. Martinez ML, Heredia MP, Delgado C. Expression of T-type Ca(2+) channels in ventricular cells from hypertrophied rat hearts. *J Mol Cell Cardiol*. 1999;31:1617–1625.
19. Ferron L, Capuano V, Ruchon Y, Deroubaix E, Coulombe A, Renaud JF. Angiotensin II signaling pathways mediate expression of cardiac T-type calcium channels. *Circ Res*. 2003;93:1241–1248.
20. Huang B, Qin D, Deng L, Boutjdir M, N E-S. Reexpression of T-type Ca2+ channel gene and current in post-infarction remodeled rat left ventricle. *Cardiovasc Res.* 2000;46:442–449.
21. Elvan A. Reexpression of T-type Ca channels after myocardial infarction: does it play a role in cardiac excitation? *Cardiovasc Res*. 2000;46:361–363.
22. Izumi T, Kihara Y, Sarai N, Yoneda T, Iwanaga Y, Inagaki K, Onozawa Y, Takenaka H, Kita T, Noma A. Reinduction of T-type calcium channels by endothelin-1 in failing hearts in vivo and in adult rat ventricular myocytes in vitro. *Circulation*. 2003;108:2530–2535.
23. Kuwahara K, Saito Y, Takano M, Arai Y, Yasuno S, Nakagawa Y, Takahashi N, Adachi Y, Takemura G, Horie M, Miyamoto Y, Morisaki T, Kuratomi S, Noma A, Fujiwara H, Yoshimasa Y, Kinoshita H, Kawakami R, Kishimoto I, Nakanishi M, Usami S, Saito Y, Harada M, Nakao K. NRSF regulates the fetal cardiac gene program and maintains normal cardiac structure and function. *EMBO J*. 2003;22:6310–6321.
24. Perez-Reyes E, Cribbs LL, Daud A, Lacerda AE, Barclay J, Williamson MP, Fox M, Rees M, Lee JH. Molecular characterization of a neuronal low-voltage-activated T-type calcium channel. *Nature*. 1998;391:896–900.
25. Cribbs LL, Lee JH, Yang J, Satin J, Zhang Y, Daud A, Barclay J, Williamson MP, Fox M, Rees M, Perez-Reyes E. Cloning and characterization of alpha1H from human heart, a member of the T-type Ca2+ channel gene family. *Circ Res*. 1998;83:103–109.
26. Lee JH, Daud AN, Cribbs LL, Lacerda AE, Pereverzev A, Klockner U, Schneider T, Perez-Reyes E. Cloning and expression of a novel member of the low voltage-activated T-type calcium channel family. *J Neurosci*. 1999;19:1912–1921.
27. Cribbs LL, Martin BL, Schroder EA, Keller BB, Delisle BP, Satin J. Identification of the t-type calcium channel (Ca(v) 3.1d) in developing mouse heart. *Circ Res.* 2001;88:403–407.
28. Niwa N, Yasui K, Opthof T, Takemura H, Shimizu A, Horiba M, Lee JK, Honjo H, Kamiya K, Kodama I. Cav3.2 subunit underlies the functional T-type Ca2+ channel in murine hearts during the embryonic period. *Am J Physiol Heart Circ Physiol*. 2004;286:H2257–H2263.
29. Mizuta E, Miake J, Yano S, Furuichi H, Manabe K, Sasaki N, Igawa O, Hoshikawa Y, Shigemasa C, Nanba E, Ninomiya H, Hidaka K, Morisaki T, Tajima F, Hisatome I. Subtype switching of T-type Ca 2+ channels from Cav3.2 to Cav3.1 during differentiation of embryonic stem cells to cardiac cell lineage. *Circ J*. 2005;69:1284–1289.

30. Mangoni ME, Traboulsie A, Leoni AL, Couette B, Marger L, Le Quang K, Kupfer E, Cohen-Solal A, Vilar J, Shin HS, Escande D, Charpentier F, Nargeot J, Lory P. Bradycardia and slowing of the atrioventricular conduction in mice lacking CaV3.1/alpha1G T-type calcium channels. *Circ Res*. 2006;98:1422–1430.
31. Chen CC, Lamping KG, Nuno DW, Barresi R, Prouty SJ, Lavoie JL, Cribbs LL, England SK, Sigmund CD, Weiss RM, Williamson RA, Hill JA, Campbell KP. Abnormal coronary function in mice deficient in alpha1H T-type Ca2+ channels. *Science*. 2003;302:1416–1418.
32. Sandmann S, Bohle RM, Dreyer T, Unger T. The T-type calcium channel blocker mibefradil reduced interstitial and perivascular fibrosis and improved hemodynamic parameters in myocardial infarction-induced cardiac failure in rats. *Virchows Arch*. 2000;436:147–157.
33. Villame J, Massicotte J, Jasmin G, Dumont L. Effects of mibefradil, a T- and L-type calcium channel blocker, on cardiac remodeling in the UM-X7.1 cardiomyopathic hamster. *Cardiovasc Drugs Ther*. 2001;15:41–48.
34. Gomora JC, Daud AN, Weiergraber M, Perez-Reyes E. Block of cloned human T-type calcium channels by succinimide antiepileptic drugs. *Mol Pharmacol*. 2001;60:1121–1132.
35. Zou Y, Yamazaki T, Nakagawa K, Yamada H, Iriguchi N, Toko H, Takano H, Akazawa H, Nagai R, Komuro I. Continuous blockade of L-type Ca2+ channels suppresses activation of calcineurin and development of cardiac hypertrophy in spontaneously hypertensive rats. *Hypertens Res*. 2002;25:117–124.
36. Cingolani E, Ramirez Correa GA, Kizana E, Murata M, Cho HC, Marban E. Gene therapy to inhibit the calcium channel beta subunit: physiological consequences and pathophysiological effects in models of cardiac hypertrophy. *Circ Res*. 2007;101:166–175.
37. Chemin J, Monteil A, Briquaire C, Richard S, Perez-Reyes E, Nargeot J, Lory P. Overexpression of T-type calcium channels in HEK-293 cells increases intracellular calcium without affecting cellular proliferation. *FEBS Lett*. 2000;478:166–172.
38. Xie X, Van Deusen AL, Vitko I, Babu DA, Davies LA, Huynh N, Cheng H, Yang N, Barrett PQ, Perez-Reyes E. Validation of high throughput screening assays against three subtypes of Ca(v)3 T-type channels using molecular and pharmacologic approaches. *Assay Drug Dev Technol*. 2007;5:191–203.
39. Wilkins BJ, Dai YS, Bueno OF, Parsons SA, Xu J, Plank DM, Jones F, Kimball TR, Molkentin JD. Calcineurin/NFAT coupling participates in pathological, but not physiological, cardiac hypertrophy. *Circ Res*. 2004;94:110–118.
40. Yasui K, Niwa N, Takemura H, Opthof T, Muto T, Horiba M, Shimizu A, Lee JK, Honjo H, Kamiya K, Kodama I. Pathophysiological significance of T-type Ca2+ channels: expression of T-type Ca2+ channels in fetal and diseased heart. *J Pharmacol Sci*. 2005;99:205–210.
41. Royer A, van Veen TA, Le Bouter S, Marionneau C, Griol-Charhbili V, Leoni AL, Steenman M, van Rijen HV, Demolombe S, Goddard CA, Richer C, Escoubet B, Jarry-Guichard T, Colledge WH, Gros D, de Bakker JM, Grace AA, Escande D, Charpentier F. Mouse model of SCN5A-linked hereditary Lenegre's disease: age-related conduction slowing and myocardial fibrosis. *Circulation*. 2005;111:1738–1746.
42. Vikstrom KL, Bohlmeyer T, Factor SM, Leinwand LA. Hypertrophy, pathology, and molecular markers of cardiac pathogenesis. *Circ Res*. 1998;82:773–778.
43. Pandya K, Kim HS, Smithies O. Fibrosis, not cell size, delineates beta-myosin heavy chain reexpression during cardiac hypertrophy and normal aging in vivo. *Proc Natl Acad Sci U S A*. 2006;103:16864–16869.
44. Horiba M, Muto T, Ueda N, Opthof T, Miwa K, Hojo M, Lee JK, Kamiya K, Kodama I, Yasui K. T-type Ca2+ channel blockers prevent cardiac cell hypertrophy through an inhibition of calcineurin-NFAT3 activation as well as L-type Ca2+ channel blockers. *Life Sci*. 2008;82:554–560.
45. Lim HW, De Windt LJ, Steinberg L, Taigen T, Witt SA, Kimball TR, Molkentin JD. Calcineurin expression, activation, and function in cardiac pressure-overload hypertrophy. *Circulation*. 2000;101:2431–2437.

Supplement Material

Materials and Methods

Animal Model of Cardiac Hypertrophy

Eight week-old adult male mice (C57BL/6, $Ca_V3.1^{-/-}$, $Ca_V3.2^{-/-}$ or NFAT-luciferase reporter-transgenic) weighing 20-25g were subjected to pressure overload by transverse aortic banding (TAB) according to the method described previously [1]. The generation of $Ca_V3.2^{-/-}$ and NFAT-luciferase reporter transgenic mice was also described previously [2, 3].

Echocardiography and Blood Pressure Measurement

An ultrasound unit (ATL HDI 5000, SonoCT) with both a 15 MHz linear and a 7 -12 MHz sector transducer was used. The animals were anesthetized for echocardiographic examination using avertin (0.33 g/kg). Short axis M-mode analysis at the level of the papillary muscle was used for measurement of the diastolic and systolic diameters of left ventricle, as well as for the measurement of wall thickness. Pulsed wave Doppler for recording the flow pattern and velocity was performed at the levels of the left ventricula r outflow tract, right ventricular outflow tract and the mitral valve tips for recording the flow pattern and velocity. The pressure gradient at the aortic banding site was measured by continuous-wave Doppler emitted by the sector transducer. All paramet ers were measured 3 times and their averages were recorded. Tail-cuff systolic blood pressure was measured in conscious mice using a Muromachi BP monitor, MK -2000 (Muromachi Kikai Co. LTD, Japan). Mice were trained in the apparatus for 3 days before data were collected.

Real-time RT-PCR

Total RNA was extracted from lysates of left ventricle or cultured neonatal myocytes using Trizol reagent (Invitrogen Corp) according to the manufacturer's protocols. To assess mRNA transcript levels by real-time RT-PCR, the first-strand cDNA was first synthesized using the high capacity reverse transcriptase kit (Applied Biosystems). TaqMan primers and probes for hypertrophy marker genes, including mouse atrium natriuretic factor (ANF), brain natriuretic peptide (BNP), α-myosin heavy chain (α-MHC), β-myosin heavy chain (β-MHC) and skeletal α-actin (α-SA) and control GAPDH, were purchased from Applied Biosystems. Real-time PCR was performed using an ABI prism 7900 sequence detection system. The fluorescent amplification curve of the product was determined, and the cycle at which the fluorescence reached a threshold was recorded (C_t) in triplicate and averaged. To control for variability in RNA quantity, the measured abundances of hypertrophic marker genes were normalized to that of GAPDH using the formula $\Delta C_t = C_{t\,(\text{Detected Genes})} - C_{t\,(\text{GAPDH})}$. The relative expression in banded hearts (normalized to WT, sham hearts) was then determined using the following relationship: gene expression = $2^{-\Delta\Delta Ct}$, where $\Delta\Delta C_t = \Delta C_t$ (banded) - ΔC_t (WT sham).

To detect $Ca_v3.1$, $Ca_v3.2$, and $Ca_v3.3$ mRNA from *in vitro* cultured neonatal myocytes stimulated by Ang II or mock, RT-PCR was performed and their expression levels were further quantified by SYBR green PCR kit (Applied Biosystems). The following Ca_v3 genes primers were used : $Ca_v3.1$: forward: 5'-CGCTGAGTCTCTC TGGTTTGTC-3', and reverse: 5'-TGCTTACATGGGACTTTTCAGA-3'; $Ca_v3.2$: forward: 5'-TGA ACCCAGAGTTTCCTCT -3',and reverse: 5'-ACAACTTCTGGT GGTGGT-3'; $Ca_v3.3$: forward: 5'-CATGAGAGCAACCAAGCA-3', and reverse:5'-AC

TCACAGTAGCCTGGCG-3'; and GAPDH: forward: 5'-GGAGCCAAACGGGTCAT CATCTC-3', and reverse: 5'-GAGGGGCCATCCACAGTCTTCT-3'. The relative expression levels of Ca_v3 genes were compared with those of GAPDH by the $2^{-\Delta\Delta Ct}$ method (normalized to mock stimulations). For both hypertrophy marker and Ca_v3 genes, the cycling conditions included in a hot start at 95 ℃ for 10 min, followed by 40 cycles at 95℃ for 15 seconds, and 60℃ for 1 min.

Fibrosis and Morphometry of Adult Hearts and Newborn Mouse Cardiomyocytes

Anesthetized mice were perfused with 20 ml 0.5% Lidocaine/ 1X PBS followed by 20ml 10% neutral buffered formalin through left ventricle of heart. Hearts were removed, fixed in 10% neutral formalin for 24 h at room temperature and embedded in paraffin for further histological analysis. Five-micrometer thick cardiac sections were cut and stained with trichrome and picro-sirius red (PSR) to detect interstitial fibrosis or stained with hematoxylin and eosin (H&E) to measure myocyte cross-sectional diameter (CSD). To visualize isolated neonatal cardiomyocytes, myocytes were identified with α-actinin antibody (Sigma-Aldrich) and nuclei were stained with 4',6-diamidino-2-phenylindole (DAPI). Myocardial interstitial fibrosis was determined by Meta Morph (version 7.1, Molecular Devices) and measurement of the muscle fiber cross-sectional diameter and morphological analysis of the neonatal cardiomyocyte surface were performed using ImagePro software (ImagePro Plus 5.1, Media Cybernetics).

Chronic Drug Infusion Study

Drug delivery was achieved by implanting an osmotic minipump (model 1002, Alzet,

Durect; Cupertino, CA) subcutaneously under anesthesia by 1.5 % isoflurane (Halocarbon, River Edge, NJ). Ang II (1.3 mg/kg per day for 14 days) or saline (0.9 % NaCl) was infused continuously. For the hypertrophy preventio n study, pumps filled with ethosuximide (0.1 mg/kg/day) or vehicle were set to deliver immediately after TAB for 14 days.

Primary Culture of Newborn Mouse Cardiomyocytes

To isolate newborn cardiomyocyte, the ventricles from 1 - to 3-day-old WT and $Ca_v3.2^{-/-}$ mice were digested by collagenase and trypsin (Worthington Biochemical Corp.). To examine the hypertrophic effects of agonists on myocytes from WT and $Ca_v3.2^{-/-}$ hearts, isolated cells were plated in dishes coated with collagen and polylysine (Sigma-Aldrich) in DMEM medium containing newborn bovine serum (10 %), penicillin (100 units/mL), streptomycin (100 μg/mL) and B-D-arabinofuranoside cytosine (17 μmol/L) for 2 days. After overnight incubation in serum -free medium, myocytes were treated with vehicle, or Ang II (100 μmol/L) for 48 hours at 37°C.

Adult Myocyte Isolation and Electrophysiological Measurements

Adult sham or banded WT and $Ca_v3.2^{-/-}$ male mice were anesthetized with 3% isoflurane. A heart was injected with cardioplegia solution via infe rior vena cava containing (in mmole/L) 20 KCl, 166.5 glucose, 3.8 $NaHCO_3$, 20 HEPES and 0.11 mg/ml heparin to stop heartbeat. It was quickly removed from the chest and retrogradely perfused through aorta at constant flow 3 ml/min for 5 min at 37 °C with Ca^{2+}-free Tyrode solution containing (in m mole/L) 120 NaCl, 5.4 KCl, 1.2 $MgSO_4$, 1.2 KH_2PO_4, 10 2,3-butanedione monoxime, 10 HEPES and 10 glucose, pH 7.4 adjusted by NaOH. Then a heart was perfused by digestion solution containing collagenase type I (0.5 mg/ml,

Sigma), protease (0.01 mg/m1, Sigma) and BSA (2.5 mg/ml) dissolved in Ca^{2+}-free Tyrode solution for ~20 min. A flaccid heart was removed from cannula and left ventricle was teased apart with forceps and passed through progressively smaller transfer pipette. The isolated ventricular myocytes were stored in the KB solution containing (in mmole/L) 30 K_2HPO_4, 5 creatine, 20 taurine, 20 glucose, 5 pyruvic acid, 85 K - glutamate, 5 $MgCl_2$, 1 EGTA and 2 Na_2ATP, pH 7.3 adjusted by KOH, before use at room temperature.

Patch electrodes were pulled from capillary glass tubing (ID 1.16 mm, Warner Instruments) on a Sutter p-97 micropipette puller (Sutter Instruments) and used with fire-polishing (Narishige MF-830). All pipettes have tip resistance 1~1.5 MΩ in a bath solution containing (in mmole/L) 145 tetraethylammonium chloride (TEA-Cl), 5 $CaCl_2$, 5 glucose, 10 HEPES, 1 $MgCl_2$, 5 CsCl and 1 4-aminopyridine and 0.01 tetrodotoxin (pH7.3 by TEA-OH, 300 mOsm). The pipette-filling solution contains (in mmole/L) 130 CsCl, 5 $MgCl_2$, 10 EGTA, 20 HEPES, 3 Mg_2ATP and 0.3 Tris-GTP (pH 7.3 by CsOH, 310 mOsm). Quiescent myocytes showing clear striation were used for the electrical recording. Whole-cell recordings were started 5 min after seal disruption and experiments were completed in 15 min. T- and L-type Ca^{2+} current were separated by applying voltage steps in 10 mV increments, with a pulse interval of 5 s, to different test potentials from a holding potential of -90 mV and -50 mV. T-type Ca^{2+} current is defined as the difference between the currents from two holding potentials. The currents were recorded at room temperature (20~22 °C) using an Axopatch 200B amplifier (Axon Instruments, Forster city), filtered at 5 kHz and digitized at 25 kHz with a Digidata 1322A data acquisition system and analyzed by pCLAMP 9.2 software.

Luciferase Reporter Assays in HEK293 Cells and Mouse Hearts

HEK293 cells were grown in DMEM medium containing newborn bovine serum (10 %), penicillin (100 units/mL) and streptomycin (100 μg/mL). PGL 4.30 (Promega) containing NFAT-luciferase reporter and pEGFP-C3 (Clontech) plasmids were transiently co-transfected with plasmids harboring human $Ca_V3.2$ or control plasmids PCMV-3tag (Strategen) into HEK293 cells using Lipofectamine 2000 (Invitrogen Corp). Cells were trypsinized and replated equally into 24-well plates 6 hours after transfection and grown in culture overnight at 37°C. They were divided into groups and pre-treated with vehicle or 1 μmole/L mibefradil for 24 hours, and were followed by treatment either with 10 mmole/L Ca^{2+} or 10 mmole/L Ca^{2+} plus mibefradil for 6 hours. Cells were harvested and the luciferase activities were determined according to the manufacturer's protocol (Promega, Madison, WI) and normalized by EGFP intensity. Luciferase activities in left ventricle lysates of WT or $Ca_V3.2^{-/-}$ NAFT-luciferase reporter mice were also measured using Promega assay kits.

Immunoprecipitation

HEK293 cells were transfected with FLAG-tagged Cav3.1 and Cav3.2 or control plasmid pCMV-3tag. Two days later, cells were lysed by cell lysis buffer containing 50 mmole/L Tris-HCL, 150 mmole/L NaCl, 1% NP-40, pH 7.4, supplemented with protease inhibitor mixture, sonicated on ice briefly, and centrifuged at 16,100 ×g for 10 min at 4°C. The supernatants were kept as cell lysates. Equal amount (5.5 mg) of cell lysates were subjected to immunoprecipitation with anti-FLAG M2 affinity gel (Sigma), followed by an overnight incubation at 4°C. After a five-times wash with wash buffer (50 mmole/L

Tris-HCL, 500 mmole/L NaCl, 1% NP-40, pH 7.4), bound proteins eluted by sample buffer (62.5 mmole/L Tris-HCl, 2% SDS, 10% glycerol, pH 6.8) were incubated for 5 min at room temperature. Five percent of 2-mercaptoethanol was added to elutes after M2 beads were removed. The rabbit monoclonal anti-calcineurin (Abcam), mouse monoclonal anti-calcineurin (BD), goat polyclonal anti-GAPDH (Santa Cruz), and HRP-conjugated anti-FLAG (Sigma) antibodies were used in western-blot analysis.

Statistical Analysis

Results are expressed as mean ± SEM. One way ANOVA repeated measurement (Turkey Test) or Student's *t*-test was used for comparison between basal data and the data with treatments at different time points within the same genotype . Kruskal-Wallis One Way Analysis of Variance on Ranks (Dunn's Method, ANOVA) was used for comparison of the variants between groups with different genotype at the certain time poin t. A probability value < 0.05 was considered statistically significant.

References

1. Hu P, Zhang D, Swenson L, Chakrabarti G, Abel ED, Litwin SE. Minimally invasive aortic banding in mice: effects of altered cardiomyocyte insulin signaling during pressure overload. *Am J Physiol Heart Circ Physiol.* 2003;285:H1261-1269.

2. Chen CC, Lamping KG, Nuno DW, Barresi R, Prouty SJ, Lavoie JL, Cribbs LL, England SK, Sigmund CD, Weiss RM, Williamson RA, Hill JA, Campbell KP. Abnormal coronary function in mice deficient in alpha1H T-type Ca2+ channels. *Science.* 2003;302:1416-1418.

3. Wilkins BJ, Dai YS, Bueno OF, Parsons SA, Xu J, Plank DM, Jones F, Kimball TR, Molkentin JD. Calcineurin/NFAT coupling participates in pathological , but not physiological, cardiac hypertrophy. *Circ Res.* 2004;94:110-118.

Online Table I. Echocardiographic Analysis of Mice Subjected to Pressure Overload

	WT		$Ca_V3.2^{-/-}$		$Ca_V3.1^{-/-}$	
	basal (n=19)	TAB (n=22)	basal (n=21)	TAB (n=22)	basal (n=7)	TAB (n=7)
HR(bpm)	481±8	459±9	492±7	474±9	453±27	424±26
LVM(mg)	104±1	140±5#	95±2	107±4*	117±4	153±5#
BW(g)	26.16±0.32	25.62±0.33	22.66±0.22*	23.56±0.32*	26.96±6.71	27.76±0.90
LVPWd(mm)	0.87±0.02	0.98±0.02#	0.80±0.01	0.85±0.21*	0.74±0.03	0.93±0.03#
LVIDd(mm)	3.47±0.03	3.60±0.05	3.45±0.03	3.52±0.06	4.11±0.12*	4.17±0.14*
LVPWs(mm)	1.26±0.02	1.42±0.03#	1.22±0.02	1.33±0.03	1.19±0.03	1.30±0.04
LVIDs(mm)	2.06±0.03	2.13±0.07	1.98±0.03	2.17±0.07	2.49±1.5*	2.71±0.14*
FS (%)	41.27±0.68	41.27±1.25	42.66±0.71	40.34±1.17	39.71±2.57	35.14±2.05
PG(m/s)		3.74±0.08		3.61±0.09		3.56±2.05
LV/BW(mg/g)	4.01±0.06	5.49±0.20#	4.24±0.09	4.57±0.15*	4.36±0.14	5.53±0.18#

Heart functions of C57B6 wild type (WT) mice, $Ca_V3.2^{-/-}$ (KO) mice and $Ca_V3.1^{-/-}$ (KO) before (basal) and at week 2 after Throcic Aortic Bading operation(TAB). HR, heart rate; LV/BW, the ratio of left ventricle to body weight; LVM, the mass of left ventricle; BW, body weight; LVPWd, left ventricular posterior wall at end diastole; LVIDd, left v entricular internal dimension at end diastole; LVPWs, left ventricular posterior wall at end systole; LVIDs, left ventricular internal dimension at end systole;FS, fraction shortening; PG, Doppler flow pressure gradiant. (#: compare basal to TAB groups; *: compare WT to KO mice.)

Supplement Material

Materials and Methods

Animal Model of Cardiac Hypertrophy

Eight week-old adult male mice (C57BL/6, $Ca_V3.1^{-/-}$, $Ca_V3.2^{-/-}$ or NFAT-luciferase reporter-transgenic) weighing 20-25g were subjected to pressure overload by transverse aortic banding (TAB) according to the method described previously [1]. The generation of $Ca_V3.2^{-/-}$ and NFAT-luciferase reporter transgenic mice was also described previously [2, 3].

Echocardiography and Blood Pressure Measurement

An ultrasound unit (ATL HDI 5000, SonoCT) with both a 15 MHz linear and a 7 -12 MHz sector transducer was used. The animals were anesthetized for echocardiographic examination using avertin (0.33 g/kg). Short axis M-mode analysis at the level of the papillary muscle was used for measurement of the diastolic and systolic diameters of left ventricle, as well as for the measurement of wall thickness. Pulsed wave Doppler for recording the flow pattern and velocity was performed at the levels of the left ventricula r outflow tract, right ventricular outflow tract and the mitral valve tips for recording the flow pattern and velocity. The pressure gradient at the aortic banding site was measured by continuous-wave Doppler emitted by the sector transducer. All paramet ers were measured 3 times and their averages were recorded. Tail-cuff systolic blood pressure was measured in conscious mice using a Muromachi BP monitor, MK -2000 (Muromachi Kikai Co. LTD, Japan). Mice were trained in the apparatus for 3 days before data were collected.

Real-time RT-PCR

Total RNA was extracted from lysates of left ventricle or cultured neonatal myocytes using Trizol reagent (Invitrogen Corp) according to the manufacturer's protocols. To assess mRNA transcript levels by real-time RT-PCR, the first-strand cDNA was first synthesized using the high capacity reverse transcriptase kit (Applied Biosystems). TaqMan primers and probes for hypertrophy marker genes, including mouse atrium natriuretic factor (ANF), brain natriuretic peptide (BNP), α-myosin heavy chain (α-MHC), β-myosin heavy chain (β-MHC) and skeletal α-actin (α-SA) and control GAPDH, were purchased from Applied Biosystems. Real-time PCR was performed using an ABI prism 7900 sequence detection system. The fluorescent amplification curve of the product was determined, and the cycle at which the fluorescence reached a threshold was recorded (C_t) in triplicate and averaged. To control for variability in RNA quantity, the measured abundances of hypertrophic marker genes were normalized to that of GAPDH using the formula $\Delta C_t = C_{t\,(\text{Detected Genes})} - C_{t\,(\text{GAPDH})}$. The relative expression in banded hearts (normalized to WT, sham hearts) was then determined using the following relationship: gene expression = $2^{-\Delta\Delta Ct}$, where $\Delta\Delta C_t = \Delta C_t$ (banded) - ΔC_t (WT sham).

To detect $Ca_v3.1$, $Ca_v3.2$, and $Ca_v3.3$ mRNA from *in vitro* cultured neonatal myocytes stimulated by Ang II or mock, RT-PCR was performed and their expression levels were further quantified by SYBR green PCR kit (Applied Biosystems). The following Ca_v3 genes primers were used : $Ca_v3.1$: forward: 5'-CGCTGAGTCTCTC TGGTTTGTC-3', and reverse: 5'-TGCTTACATGGGACTTTTCAGA-3'; $Ca_v3.2$: forward: 5'-TGA ACCCAGAGTTTCCTCT -3',and reverse: 5'-ACAACTTCTGGT GGTGGT-3'; $Ca_v3.3$: forward: 5'-CATGAGAGCAACCAAGCA-3', and reverse:5'-AC

TCACAGTAGCCTGGCG-3'; and GAPDH: forward: 5'-GGAGCCAAACGGGTCAT CATCTC-3', and reverse: 5'-GAGGGGCCATCCACAGTCTTCT-3'. The relative expression levels of Ca_v3 genes were compared with those of GAPDH by the $2^{-\Delta\Delta Ct}$ method (normalized to mock stimulations). For both hypertrophy marker and Ca_v3 genes, the cycling conditions included in a hot start at 95 ℃ for 10 min, followed by 40 cycles at 95℃ for 15 seconds, and 60℃ for 1 min.

Fibrosis and Morphometry of Adult Hearts and Newborn Mouse Cardiomyocytes

Anesthetized mice were perfused with 20 ml 0.5% Lidocaine/ 1X PBS followed by 20ml 10% neutral buffered formalin through left ventricle of heart. Hearts were removed, fixed in 10% neutral formalin for 24 h at room temperature and embedded in paraffin for further histological analysis. Five-micrometer thick cardiac sections were cut and stained with trichrome and picro-sirius red (PSR) to detect interstitial fibrosis or stained with hematoxylin and eosin (H&E) to measure myocyte cross-sectional diameter (CSD). To visualize isolated neonatal cardiomyocytes, myocytes were identified with α-actinin antibody (Sigma-Aldrich) and nuclei were stained with 4',6-diamidino-2-phenylindole (DAPI). Myocardial interstitial fibrosis was determined by Meta Morph (version 7.1, Molecular Devices) and measurement of the muscle fiber cross-sectional diameter and morphological analysis of the neonatal cardiomyocyte surface were performed using ImagePro software (ImagePro Plus 5.1, Media Cybernetics).

Chronic Drug Infusion Study

Drug delivery was achieved by implanting an osmotic minipump (model 1002, Alzet,

Durect; Cupertino, CA) subcutaneously under anesthesia by 1.5 % isoflurane (Halocarbon, River Edge, NJ). Ang II (1.3 mg/kg per day for 14 days) or saline (0.9 % NaCl) was infused continuously. For the hypertrophy preventio n study, pumps filled with ethosuximide (0.1 mg/kg/day) or vehicle were set to deliver immediately after TAB for 14 days.

Primary Culture of Newborn Mouse Cardiomyocytes

To isolate newborn cardiomyocyte, the ventricles from 1 - to 3-day-old WT and $Ca_v3.2^{-/-}$ mice were digested by collagenase and trypsin (Worthington Biochemical Corp.). To examine the hypertrophic effects of agonists on myocytes from WT and $Ca_v3.2^{-/-}$ hearts, isolated cells were plated in dishes coated with collagen and polylysine (Sigma-Aldrich) in DMEM medium containing newborn bovine serum (10 %), penicillin (100 units/mL), streptomycin (100 μg/mL) and B-D-arabinofuranoside cytosine (17 μmol/L) for 2 days. After overnight incubation in serum -free medium, myocytes were treated with vehicle, or Ang II (100 μmol/L) for 48 hours at 37°C.

Adult Myocyte Isolation and Electrophysiological Measurements

Adult sham or banded WT and $Ca_v3.2^{-/-}$ male mice were anesthetized with 3% isoflurane. A heart was injected with cardioplegia solution via infe rior vena cava containing (in mmole/L) 20 KCl, 166.5 glucose, 3.8 $NaHCO_3$, 20 HEPES and 0.11 mg/ml heparin to stop heartbeat. It was quickly removed from the chest and retrogradely perfused through aorta at constant flow 3 ml/min for 5 min at 37 °C with Ca^{2+}-free Tyrode solution containing (in m mole/L) 120 NaCl, 5.4 KCl, 1.2 $MgSO_4$, 1.2 KH_2PO_4, 10 2,3-butanedione monoxime, 10 HEPES and 10 glucose, pH 7.4 adjusted by NaOH. Then a heart was perfused by digestion solution containing collagenase type I (0.5 mg/ml,

Sigma), protease (0.01 mg/m1, Sigma) and BSA (2.5 mg/ml) dissolved in Ca^{2+}-free Tyrode solution for ~20 min. A flaccid heart was removed from cannula and left ventricle was teased apart with forceps and passed through progressively smaller transfer pipette. The isolated ventricular myocytes were stored in the KB solution containing (in mmole/L) 30 K_2HPO_4, 5 creatine, 20 taurine, 20 glucose, 5 pyruvic acid, 85 K - glutamate, 5 $MgCl_2$, 1 EGTA and 2 Na_2ATP, pH 7.3 adjusted by KOH, before use at room temperature.

Patch electrodes were pulled from capillary glass tubing (ID 1.16 mm, Warner Instruments) on a Sutter p-97 micropipette puller (Sutter Instruments) and used with fire-polishing (Narishige MF-830). All pipettes have tip resistance 1~1.5 MΩ in a bath solution containing (in mmole/L) 145 tetraethylammonium chloride (TEA-Cl), 5 $CaCl_2$, 5 glucose, 10 HEPES, 1 $MgCl_2$, 5 CsCl and 1 4-aminopyridine and 0.01 tetrodotoxin (pH7.3 by TEA-OH, 300 mOsm). The pipette-filling solution contains (in mmole/L) 130 CsCl, 5 $MgCl_2$, 10 EGTA, 20 HEPES, 3 Mg_2ATP and 0.3 Tris-GTP (pH 7.3 by CsOH, 310 mOsm). Quiescent myocytes showing clear striation were used for the electrical recording. Whole-cell recordings were started 5 min after seal disruption and experiments were completed in 15 min. T- and L-type Ca^{2+} current were separated by applying voltage steps in 10 mV increments, with a pulse interval of 5 s, to different test potentials from a holding potential of -90 mV and -50 mV. T-type Ca^{2+} current is defined as the difference between the currents from two holding potentials. The currents were recorded at room temperature (20~22 °C) using an Axopatch 200B amplifier (Axon Instruments, Forster city), filtered at 5 kHz and digitized at 25 kHz with a Digidata 1322A data acquisition system and analyzed by pCLAMP 9.2 software.

Luciferase Reporter Assays in HEK293 Cells and Mouse Hearts

HEK293 cells were grown in DMEM medium containing newborn bovine serum (10 %), penicillin (100 units/mL) and streptomycin (100 μg/mL). PGL 4.30 (Promega) containing NFAT-luciferase reporter and pEGFP-C3 (Clontech) plasmids were transiently co-transfected with plasmids harboring human $Ca_V3.2$ or control plasmids PCMV-3tag (Strategen) into HEK293 cells using Lipofectamine 2000 (Invitrogen Corp). Cells were trypsinized and replated equally into 24-well plates 6 hours after transfection and grown in culture overnight at 37°C. They were divided into groups and pre-treated with vehicle or 1 μmole/L mibefradil for 24 hours, and were followed by treatment either with 10 mmole/L Ca^{2+} or 10 mmole/L Ca^{2+} plus mibefradil for 6 hours. Cells were harvested and the luciferase activities were determined according to the manufacturer's protocol (Promega, Madison, WI) and normalized by EGFP intensity. Luciferase activities in left ventricle lysates of WT or $Ca_V3.2^{-/-}$ NAFT-luciferase reporter mice were also measured using Promega assay kits.

Immunoprecipitation

HEK293 cells were transfected with FLAG-tagged Cav3.1 and Cav3.2 or control plasmid pCMV-3tag. Two days later, cells were lysed by cell lysis buffer containing 50 mmole/L Tris-HCL, 150 mmole/L NaCl, 1% NP-40, pH 7.4, supplemented with protease inhibitor mixture, sonicated on ice briefly, and centrifuged at 16,100 ×g for 10 min at 4°C. The supernatants were kept as cell lysates. Equal amount (5.5 mg) of cell lysates were subjected to immunoprecipitation with anti-FLAG M2 affinity gel (Sigma), followed by an overnight incubation at 4°C. After a five-times wash with wash buffer (50 mmole/L

Tris-HCL, 500 mmole/L NaCl, 1% NP-40, pH 7.4), bound proteins eluted by sample buffer (62.5 mmole/L Tris-HCl, 2% SDS, 10% glycerol, pH 6.8) were incubated for 5 min at room temperature. Five percent of 2-mercaptoethanol was added to elutes after M2 beads were removed. The rabbit monoclonal anti-calcineurin (Abcam), mouse monoclonal anti-calcineurin (BD), goat polyclonal anti-GAPDH (Santa Cruz), and HRP-conjugated anti-FLAG (Sigma) antibodies were used in western-blot analysis.

Statistical Analysis

Results are expressed as mean ± SEM. One way ANOVA repeated measurement (Turkey Test) or Student's *t*-test was used for comparison between basal data and the data with treatments at different time points within the same genotype . Kruskal-Wallis One Way Analysis of Variance on Ranks (Dunn's Method, ANOVA) was used for comparison of the variants between groups with different genotype at the certain time poin t. A probability value < 0.05 was considered statistically significant.

References

1. Hu P, Zhang D, Swenson L, Chakrabarti G, Abel ED, Litwin SE. Minimally invasive aortic banding in mice: effects of altered cardiomyocyte insulin signaling during pressure overload. *Am J Physiol Heart Circ Physiol.* 2003;285:H1261-1269.

2. Chen CC, Lamping KG, Nuno DW, Barresi R, Prouty SJ, Lavoie JL, Cribbs LL, England SK, Sigmund CD, Weiss RM, Williamson RA, Hill JA, Campbell KP. Abnormal coronary function in mice deficient in alpha1H T-type Ca2+ channels. *Science.* 2003;302:1416-1418.

3. Wilkins BJ, Dai YS, Bueno OF, Parsons SA, Xu J, Plank DM, Jones F, Kimball TR, Molkentin JD. Calcineurin/NFAT coupling participates in pathological , but not physiological, cardiac hypertrophy. *Circ Res.* 2004;94:110-118.

Online Table I. Echocardiographic Analysis of Mice Subjected to Pressure Overload

	WT		$Ca_v3.2^{-/-}$		$Ca_v3.1^{-/-}$	
	basal (n=19)	TAB (n=22)	basal (n=21)	TAB (n=22)	basal (n=7)	TAB (n=7)
HR(bpm)	481±8	459±9	492±7	474±9	453±27	424±26
LVM(mg)	104±1	140±5#	95±2	107±4*	117±4	153±5#
BW(g)	26.16±0.32	25.62±0.33	22.66±0.22*	23.56±0.32*	26.96±6.71	27.76±0.90
LVPWd(mm)	0.87±0.02	0.98±0.02#	0.80±0.01	0.85±0.21*	0.74±0.03	0.93±0.03#
LVIDd(mm)	3.47±0.03	3.60±0.05	3.45±0.03	3.52±0.06	4.11±0.12*	4.17±0.14*
LVPWs(mm)	1.26±0.02	1.42±0.03#	1.22±0.02	1.33±0.03	1.19±0.03	1.30±0.04
LVIDs(mm)	2.06±0.03	2.13±0.07	1.98±0.03	2.17±0.07	2.49±1.5*	2.71±0.14*
FS (%)	41.27±0.68	41.27±1.25	42.66±0.71	40.34±1.17	39.71±2.57	35.14±2.05
PG(m/s)		3.74±0.08		3.61±0.09		3.56±2.05
LV/BW(mg/g)	4.01±0.06	5.49±0.20#	4.24±0.09	4.57±0.15*	4.36±0.14	5.53±0.18#

Heart functions of C57B6 wild type (WT) mice, $Ca_v3.2^{-/-}$ (KO) mice and $Ca_v3.1^{-/-}$ (KO) before (basal) and at week 2 after Throcic Aortic Bading operation(TAB). HR, heart rate; LV/BW, the ratio of left ventricle to body weight; LVM, the mass of left ventricle; BW, body weight; LVPWd, left ventricular posterior wall at end diastole; LVIDd, left v entricular internal dimension at end diastole; LVPWs, left ventricular posterior wall at end systole; LVIDs, left ventricular internal dimension at end systole;FS, fraction shortening; PG, Doppler flow pressure gradiant. (#: compare basal to TAB groups; *: compare WT to KO mice.)